Investigation of Pt/Ti bilayer metallization on silicon for ferroelectric thin film integration

Kondepudy Sreenivas, Ian Reaney, Thomas Maeder and Nava Setter

Département des Matériaux, Laboratoire de Céramique, École Polytechnique Fédérale de Lausanne, CH-1015 Lausanne, Switzerland

Chennupati Jagadish and Robert G. Elliman

Department of Electronic Materials Engineering, Research School of Physical Sciences and Engineering, Australian National University, Canberra ACT 0200, Australia

Original version: Journal of Applied Physics 75 (1), 232-239, 1994.
http://hdl.handle.net/10.1063/1.355889

Abstract

The stabilities of Pt/Ti bilayer metallizations in an oxidizing atmosphere have been investigated with several thicknesses of interfacial Ti-bonding layers. Reactions in the Pt/Ti/SiO_2/Si interface were examined as a function of various annealing conditions in the temperature range 200-800°C by using Rutherford backscattering spectrometry, Auger electron spectroscopy, x-ray diffraction, and transmission electron microscopy. Thermal treatment in oxygen was found to cause rapid oxidation of the Ti layer, accompanied by the migration of Ti into the Pt film. Diffusion of oxygen through the Pt grain boundaries was mainly responsible for the adverse reactions at the interface and loss of mechanical integrity. Thin Ti (10 nm) layers resulted in the depletion of the interfacial bonding layer causing serious adhesion problems, whereas thicker Ti films (100 nm) caused the formation of TiO_{2-x} in the Pt-grain boundaries, ultimately encapsulating the Pt surface with an insulating TiO_2 layer. Improved stability and adhesion in the Pt/Ti bilayer metallization compatible with ferroelectric thin film processing, were achieved by incorporating well reacted thin TiO_2, layers *in situ*, and depositing Pt films at a high temperature.

1. Introduction

Integration of ferroelectric thin film capacitors onto silicon demands a stable metallization.' This is primarily due to the high processing temperatures encountered in the synthesis of ferroelectric oxide films. The prerequisites for a "good" metallization include: strong adhesion, resistance to oxidation, and etchability compatible with standard electrode patterning techniques. The metallization should possess good electrical conductivity, produce a clean interface with the ferroelectric film, and finally, since it serves the dual purpose of providing a bottom electrical contact and as a final surface upon which the ferroelectric film grows, its structure and composition should promote the required crystal growth in the deposited ferroelectric film.'.

Currently, various electrode materials, ranging from polycrystalline metal films to complex conducting oxides, are being studied [3-5]. Problems relating to the preparation of different electrode materials (Pt, Pt/Ti, RuO_2, ReO_3, $CoSi_2$,/Si_3N_4) and their compatibility with ferroelectric lead zirconate titanate (PZT) thin films were reviewed by Hren *et al*. [6]. Compatibility of various diffusion barriers (TiN_x, TiO_x, ZrN, and ZrO_x) for PZT deposited on silicon was evaluated by Parikh et al. [7] and interface reactions in SiO_2/PZT and Pt/PZT structures were studied by Roy and Etzold [8] using Rutherford backscattering spectrometry (RBS). Thin metallic films deposited directly on silicon have been shown to either oxidize, peel away, or form silicides [9]. Silicon wafers passivated with SiO_2/Si_3N_4 barrier layers are being used in combination with platinum films that are relatively stable in an oxidizing atmosphere. However, since platinum does not easily bond well to SiO_2, a thin layer of titanium is employed to promote adhesion [10]. At present, Pt/Ti bilayer metallizations on SiO_2 are being widely used for ferroelectric thin film integration.

Lately several degradation phenomena such as poor adhesion, degradation of ferroelectric thin film properties such as aging and fatigue, hillock growth, and diffusion of lead though platinum has been observed when ferroelectric lead zirconate titanate thin (PZT) films are interfaced with Pt/Ti bilayers [4,6]. The morphology and orientation of ferroelectric thin films is also influenced by the underlying Pt/Ti metallization [11,12]. Detailed studies on the stability of Pt/Ti bilayer metallizations in an oxidizing ambient have scarcely been reported. Large variations in the thicknesses of Pt and Ti layers listed in Table I have been attempted [12-22]. Recent studies [13,14,23] on the stability of Pt/Ti bilayers in an oxidizing atmosphere pointed out a potential problem arising due to the oxidation of the intermediate Ti-bonding layer, and its diffusion into the Pt film. Some plausible solutions have been suggested, such as the need for thin Pt/Ti (80/10 nm) layers, the necessity for an annealing treatment in air before use [13] or the use of thick Ti layers (100 nm) [14]. However, such methods have been found to be partially successful. Ferroelectric thin films prepared by sputtering, sol gel, and chemical vapor deposition techniques undergo a specific thermal treatment that varies in time and temperature, and can therefore directly affect the stability of the underlying metal layers. Thermal stability of Pt/Ti metallizations depends on the Pt microstructure, Pt/Ti interface, stress in the Pt films, and adhesion at the Ti-SiO_2 interface. These factors are purely dependent on the Pt/Ti growth conditions. For improved stability in oxygen, the ideal thicknesses, the qualities required in the bonding layer, and the basic interface reactions, have, however, not been studied in detail.

In the present article we investigate Pt/Ti bilayer metallizations deposited onto SiO_2 surfaces under various growth conditions. Adverse reactions occurring in the intermediate Ti layer and its effects on adhesion are shown to be significant. Finally, appropriate modifications in the growth conditions resulting in the development of a stable metallization are described.

Table I. Variations in the Pt/Ti bilayer metallizations deposited on silicon.

Passivation layer (thickness in nm)	Metallization (thickness in nm)		Deposition technique	Reference No.
	Platinum	Titanium		
SiO_2	*Pt-Ti alloy*[a] *(Ti/Pt =0.02-0.17)*		co-sputtering	12
SiO_2 (500)	140	100	sputtering	14
SiO_2	Pt[a]	TiO_2[a]	sputtering	15
SiO_2	100	100	evaporation	16
SiO_2 derived from-TEOS[b] (600)	200	50	dc sputtering	17
SiO_2 (100) + diffusion barrier (110)	100	150	sputtering	18
SiO_2 (400)	150	15	e-beam evaporation	19
SiO_2 (100)	100	20	sputtering	20
SiO_2 (1000)	150	20	sputtering	21
SiO_2 (500)	200	20	dc magnetron sputtering	22

(a) Thicknesses not mentioned. (b) Tetraethylorthosilicate.

2. Experiment

2.1. Preparation of the metallizations

Platinum and titanium films were deposited onto <l00> oriented silicon substrates, passivated with a thermally grown silicon dioxide (SiO_2) layer of two different thicknesses, 100 or 1000 nm. The metal films were grown by a dc magnetron sputtering technique using a Nordiko 2000 sputter system. The substrate surface (SiO_2/silicon) was cleaned *in situ* using a rf sputter cleaning procedure prior to film deposition.

Pt/Ti bilayer metallizations were fabricated by a sequential deposition process in a single pump down cycle without breaking the vacuum. The thicknesses of the metal films were typically in the range 10-100 nm as determined by step height measurements using a Tencor Instruments thin film profilometer, RRS, and transmission electron microscopy (TEM) measurements. Films were prepared at different substrate temperatures ranging from 200 to 650°C.

RRS with 2.0 MeV He^+ ions was employed to study the thermal stability, stoichiometry, and depth distribution of thin films. The beam was incident normal to the sample surface and detected at a scattering angle of 165°. Analysis of the KBS spectra was performed using the RUMP software package [24]. A Siemen's x-ray diffraction (XRD) unit with a CuK_α, source was employed to identify the phases of the inter-diffused reactions. The Auger electron spectroscopy (AES) depth profiles were acquired in a Perkin Elmer (PE 5500) scanning Auger instrument equipped with a differentially pumped ion gun. The electron beam was set at 100 nA and 3 keV, while the samples were sputtered with a 2 keV Ar ion beam at 10 mPa argon pressure. The ion beam was rastered over an area of 2×2 mm^2 and the AES depth profiles are shown as peak-to-peak heights of the derivative AES signals versus sputter time. Transverse cross section and plan sections of the samples were prepared and examined using a Philips EM330 and CM20 transmission electron microscope. The CM20 was equipped with an energy dispersive x-ray (EDX) detector and a Sun "Voyager" work station to process the spectra.

2.2. Annealing

Annealing in vacuum was carried out in the sputtering chamber at a base pressure of $1.33\times l0^{-4}$ Pa, and annealing in air for extended hours was done in a conventional box furnace at atmospheric pressure. A Process Products Corporation rapid thermal processor (RTP) was used for short annealing times in oxygen. In the initial experiments the annealing temperatures in oxygen were kept identical to those encountered during our ferroelectric PZT thin film fabrication by a sputter deposition technique [25]. This includes thermal treatment at two different stages: (1) during film deposition (200°C for 5-8 h) in oxygen at 5.33 Pa, and (b) post deposition annealing (650°C for 30 s) in a rapid thermal annealing (RTA) system. The observed interface reactions with respect to different Ti layer thick- nesses are discussed in the following discussion.

3. Results and discussion

3.1. Thin Ti layers

Figures 1(a), 1(b), and 1(c) compare the RBS spectra measured on the as-deposited and annealed Pt/Ti bilayer metallizations which have a 10 nm thick titanium layer. The spectra show distinct, clearly resolved signals from Ti and Pt as well as a signal from the underlying SiO_2 layer and the Si substrate. Comparison of the spectra shows that there is little change in the sample structure [Fig. 1(b)] after annealing at 200°C. for 8 h in pure oxygen at a pressure of 5.33 Pa in the sputtering chamber. However, diffusion of Ti at 650°C for 30 s is apparent from the broadening of the Ti peak in Fig. 1(c), as well as from the small changes in the yield of the Pt peak. Detailed analysis shows that the Ti has become redistributed throughout the Pt layer and that a fraction has accumulated at, or near, the surface. A typical problem encountered with thin Ti bonding layers (10 nm thickness) is that due to the observed migration of Ti, the structure no longer retains the required bonding material, resulting in a loss of adhesion.

Figures 2(a) and 2(b) are transmission electron micrographs in plan section showing the as-deposited metallization, and the same sample annealed for 8 h at 200°C in O_2 and 30 s at 650°C by RTA. The as-deposited sample, Fig. 2(a), has a dense microstructure in the platinum film with a grain size of approximately 50 nm. After undergoing the described heat treatments the sample exhibits grain growth (100 nm grain size) as seen in Fig. 2(b) and also exhibits pockets of a second phase at the Pt-grain boundaries. Energy dispersive x-ray (EDX) analyses confirmed that these pockets were Ti-rich, and high resolution electron microscopy identified some of the phases as rutile TiO_2. It is suspected that various phases may be present with the general nonstoichiometric formula of TiO_{2-x} where x can be equal to 0.

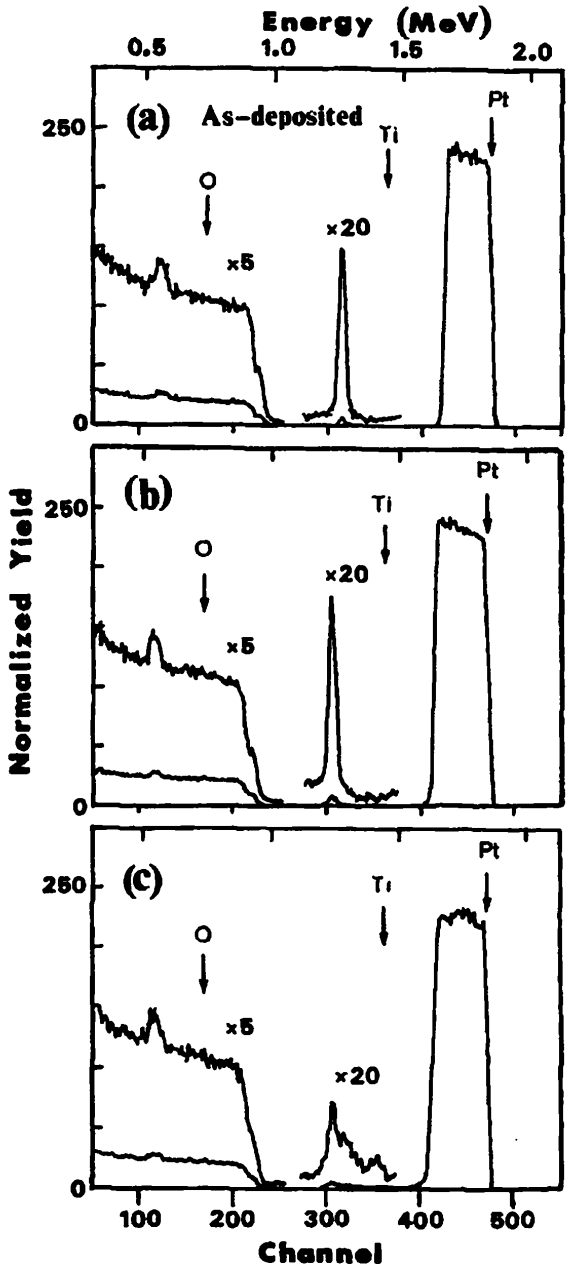

Fig 1. RBS spectra of Pt/Ti/SiO_2/Si structure with thickness of Ti = 10 nm. (a) as-deposited, (b) annealed in O_2 (5.33 Pa) at 200°C for 8 h, (c) annealed in O_2 at 200°C for 8 h, and 650°C for 30 s in O_2 (RTA). Thickness (nm): Pt= 135, SiO_2 = 100.

The expected reactions are well known in the literature on Ti/SiO_2 interface studies, and on the oxidation mechanisms in titanium. Annealing temperatures around 650°C have been found to out-diffuse oxygen atoms due to SiO_2 dissociation which dissolve into the region of the bilayer metal films [26]. The high partial pressure of O_2, and the strong affinity between Ti and oxygen seems adequate to cause its short circuit-diffusion along the Pt-grain boundaries. Considering that the solubility and diffusion rate of O_2 in bulk platinum [27] which are very low (at 500°C, $E_d > 53$ kcal/mole and $D = 10^{-21}$ $cm^2 \cdot s^{-1}$), the thermodynamic driving force for the diffusion of Ti seems to be due to the formation of a reduced oxide (TiO_{2-x}) at the interface. At high temperatures and oxygen partial pressures, Ti interstitials are the most likely defects to dominate the diffusion mechanism in a reduced TiO_{2-x} layer compared with a well reacted TiO_2 layer [28].

3.2. Thick Ti layers

The effects of annealing in oxygen with further increase in the thickness of the Ti layer to 35 nm were qualitatively similar to results presented in Fig. 1. After the high temperature anneal, Ti was redistributed throughout the Pt film, accumulating at some depth (60 nm) beneath the surface. This is evident from both the Ti signal and the Pt signal in Fig. 3 (curve 7C), the latter showing a reduced height and increased width as well as yield variation. The changes in the Pt signal suggest that the layer contains elements other than Pt and Ti, and are consistent with the film containing both Ti and O in the form of TiO_{2-x}. A systematic study performed by increasing the annealing temperature in steps (500, 600, and 700°C) shown in Fig. 3, indicated that Ti diffusion occurred after annealing at 500°C for 30 s.

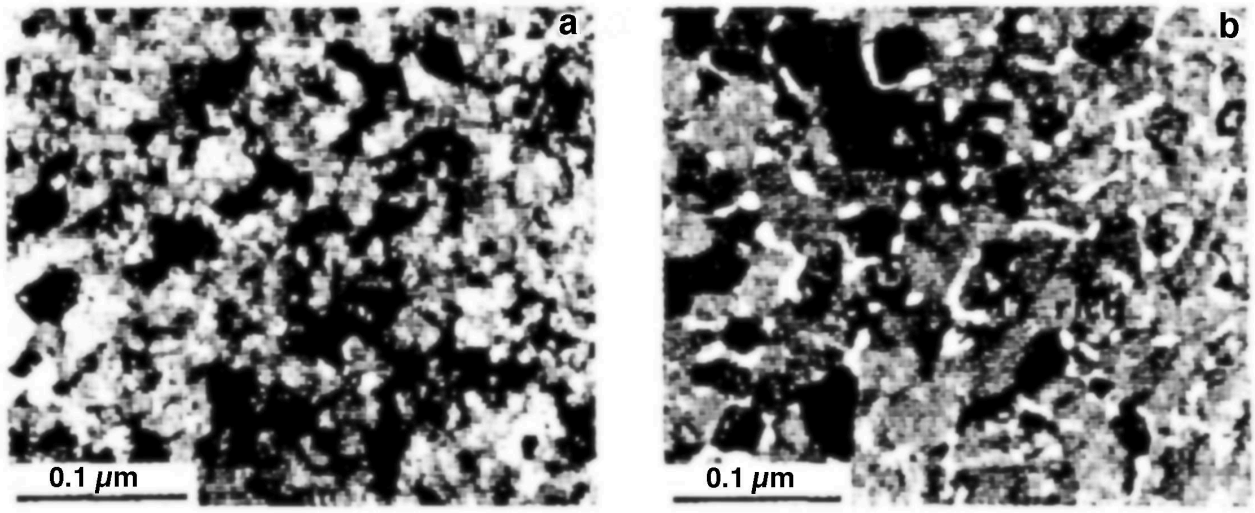

Fig 2. TEM images showing a plan section through the Pt layer in the Pt/Ti/SiO_2/Si structure (a) as-deposited and (b) annealed for 8 h at 200 "C and 650°C for 30 s in O_2. Pockets of second phase and a larger grain size are observed in (b).

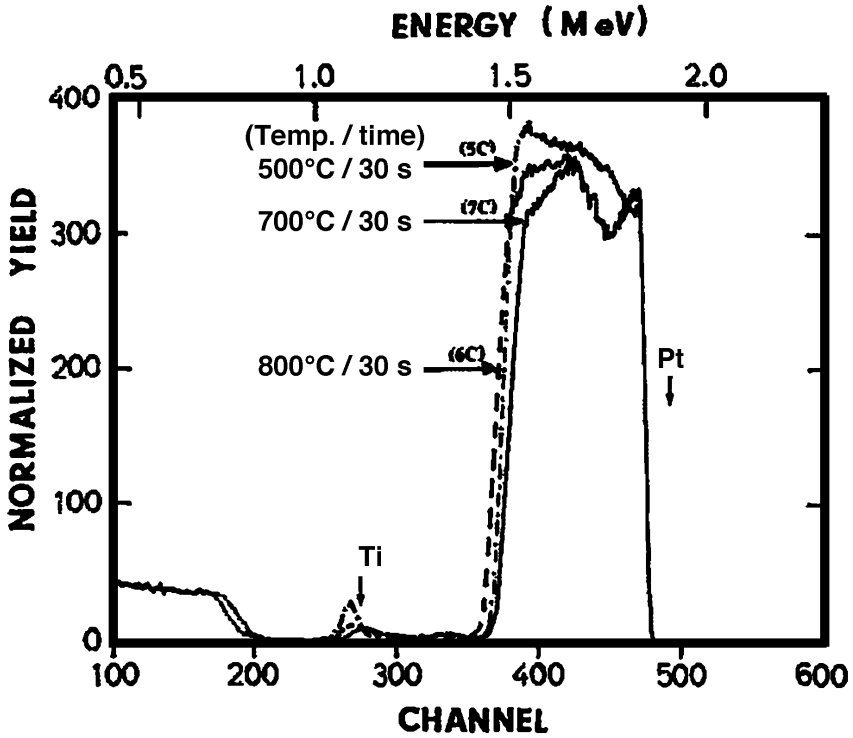

Fig 3. Evolution of the RRS spectra from Pt/Ti/SiO_2/Si samples with Ti = 35 nm showing the effects of increasing annealing temperatures in oxygen.

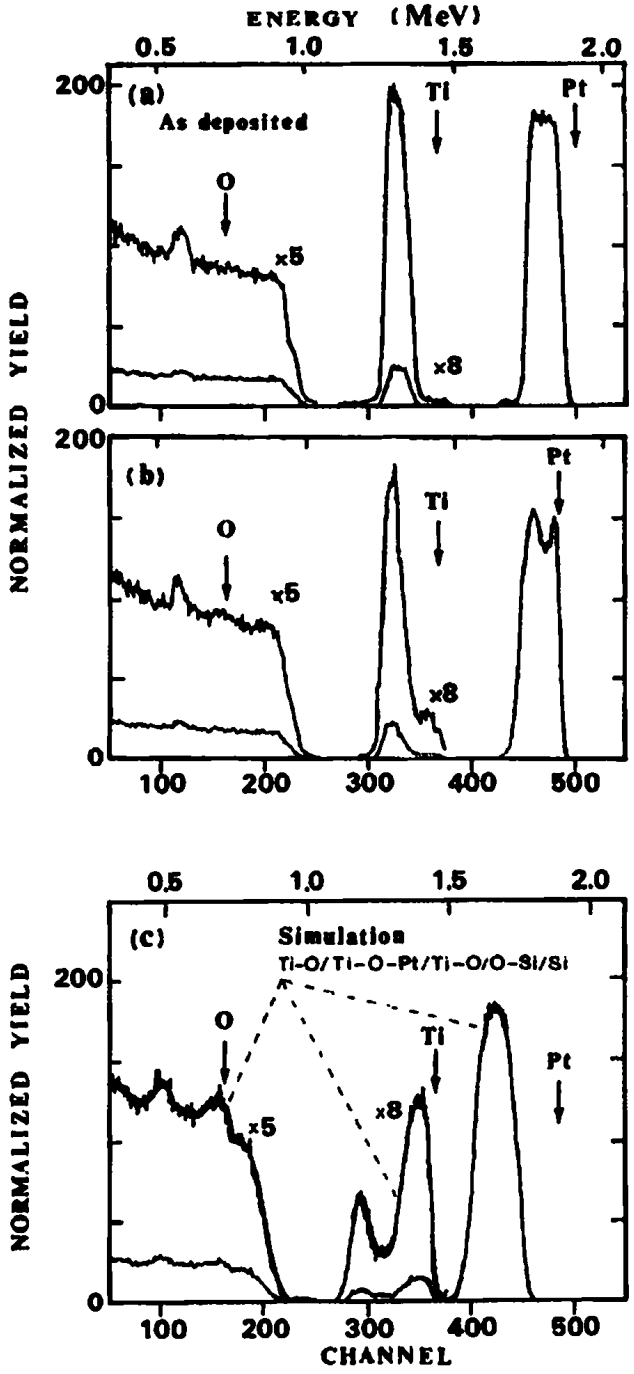

Fig 4. RBS spectra of Pt/Ti/SiO_2/Si with Ti = 100 nm, (a) as-deposited, (b) annealed in O_2 at 200°C for 8 h, (c) annealed in O_2 at 700°C for 2 min, and simulation of the spectra. Thickness (nm) : Pt = 80, SiO_2 = 100.

The thickness of the Ti-bonding layer was further increased to 100 nm. Figures 4(a), 4(b), and 4(c) show the RRS spectra obtained from the as deposited and annealed Pt/Ti samples. Although the Pt layer is considerably thinner (80 nm), annealing in oxygen produced significant changes. The RBS spectrum shown in Fig. 4(c) for the sample annealed at 700°C for 2 min, reveals that the sample has a surface layer containing Ti and O, probably in the form of TiO_2, and the underlying Pt film contains high concentrations of Ti and O. A cursory optical examination of the sample revealed the loss of metallic surface reflection of Pt films upon annealing, and they had become blue, or purple in color. The platinum surface was no longer electrically conducting, but was insulating, However, the platinum layer underneath was still conductive, implying that it was encapsulated by an insulating TiO_2 film. The present observations are in agreement with the observations of Scott *et al.* [29], where the formation of a rutile TiO_2 as a reaction product at the Pt/Ti interfaces was suggested as a potential cause for enhancing the fatigue mechanisms in PZT films [29]. However, it needs to be established further whether the TiO_{2-x} surface layers exist uniformly, or only at the Pt grain boundaries, when the metallization is processed along with a ferroelectric PZT thin film.

The RBS spectrum from the sample annealed at 700°C for 2 min [Fig. 4(c)] was simulated by assuming the following sample structure: a surface layer of TiO_2 of average thickness 366 nm (1150×10^{15} atoms/cm^2), followed by a layer containing a mixture of 40 at. % TiO^2 and 60 at. % Pt of average thickness 162 nm (850×10^{15} atoms/cm^2), a layer of Ti of average thickness 15 nm (85×10^{15} atoms/cm^2), a layer of TiO_2 of average thickness 32 nm (100×10^{15} atoms/cm^2), then a layer of SiO_2, and finally a layer of Si.

The simulation also suggests that the interfaces between layers 1 and 2, and 2 and 3 are rough, with a full-width-half-maximum (FWHM) roughness of 84 nm (350×10^{15} atoms/cm^2) between layers 1 and 2, and 35 nm (150×10^{15} atoms/cm^2) between layers 2 and 3. The experimental and theoretical spectra are seen to be in good agreement [Fig. 4(c)] but it must be noted that the fit is not unique, and is based on what are believed to be plausible layer structures. All simulations were performed with layer thicknesses in atoms/cm^2. These units were converted to nm by assuming the bulk atomic densities of TiO_2 and Pt. Layer thicknesses will therefore be inaccurate if film densities are different from bulk values, for example if the film is porous. The RBS spectrum from a sample annealed at 700°C for 30 s (curve 7C in Fig. 3) was also simulated, but the complexity of simulating the depth dependent Ti and O distributions resulted in too many variables for a reliable fit.

Figure 5 compares the x-ray diffractograms of the as-deposited and annealed Pt/Ti metallizations with a Ti thickness of 100 nm. As-deposited Pt/Ti films revealed a strong (111) orientation for the Pt layer. However, annealing at 700°C for 2 min in oxygen altered the crystallographic orientation of the Pt causing the (200) peak to increase in intensity. Further annealing at 800°C for 2 min in oxygen showed additional peaks corresponding to rutile TiO_2, thus confirming the presence of a surface layer of TiO_2 on the Pt film. Figures 6(a) and 6(b) are transmission electron micrographs showing parts of a cross section of (a) an as-deposited metallization with a Ti layer (100 nm thick) and (b) the sample annealed in O_2 at 800°C for 2 min. In Fig. 6(a), the Ti layer has a columnar grain structure and a sharp interface with the Pt film. There appears to be a thin layer between the Ti and SiO_2 where Ti begins to reduce SiO_2. In Fig. 6(b) the interfaces between the various layers are no longer well defined upon annealing. At the surface of the Pt film, a layer is present which was identified as TiO_2 by electron diffraction and EDX analysis, and is consistent with the observations made through XRD and the RBS analysis. The Pt layer has become rough and uneven, and the original orientation of the Pt has been disrupted by the nucleation and growth of TiO_{2-x} within the layer. This would explain the appearance of the additional Pt (200) peak observed in the XRD spectra. The microstructure of the layer below the Pt consists of several phases containing Si, Ti, Pt, and O. It is proposed that a mélange of oxides and silicates is present in this region. Figure 7 shows a scanning electron micrograph of the Pt/Ti bilayer metallization in which the Pt surface is completely covered by a rough, granular TiO_2 layer, and loss of adhesion is seen in the form of spherical delaminated regions.

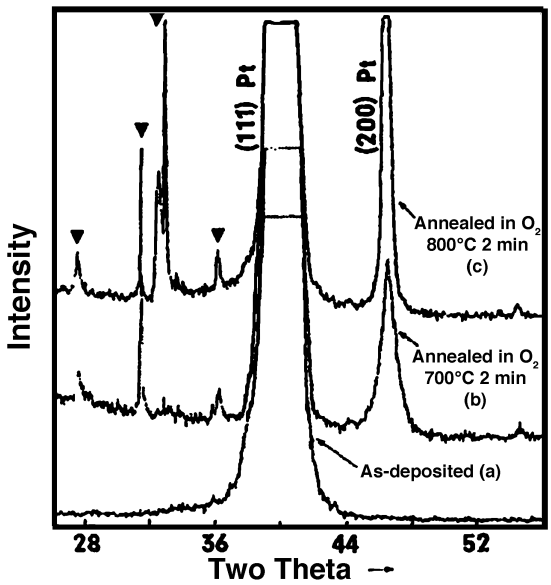

Fig 5. X-ray diffractograms of the Pt/Ti/SiO_2/Si structure with thickness of Ti = 100 nm. Comparison of as-deposited and oxygen annealed samples. Peaks corresponding to TiO_2 are denoted by ▼.

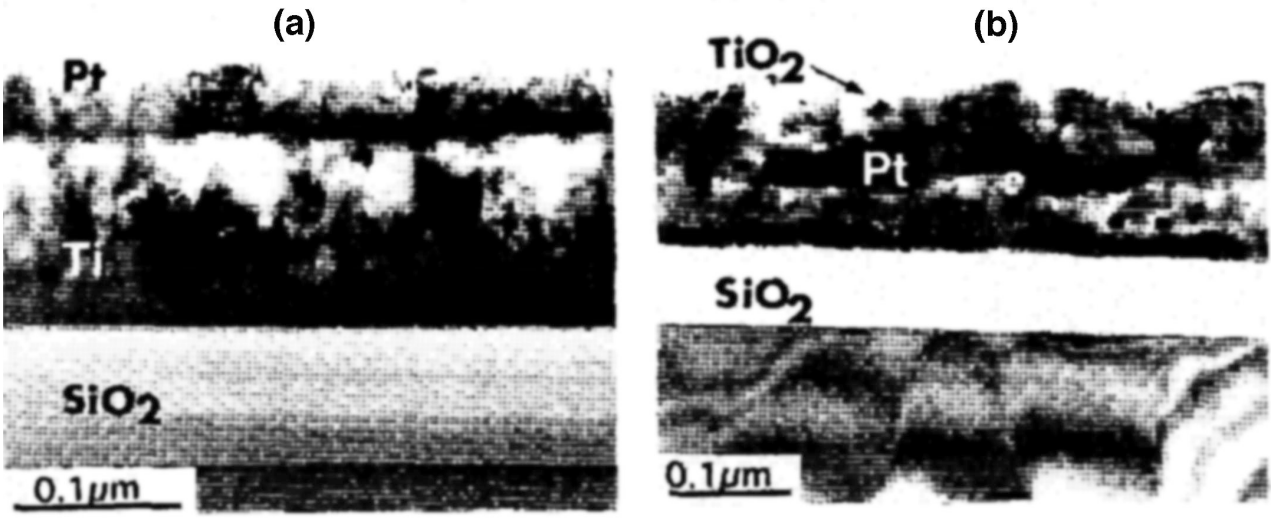

Fig 6. Transmission electron micrographs which show parts of transverse sections through the Pt/Ti/SiO_2/Si interface with thickness Ti = 100 nm: (a) as-deposited metallization and (b) sample annealed in O_2 (800°C for 2 min).

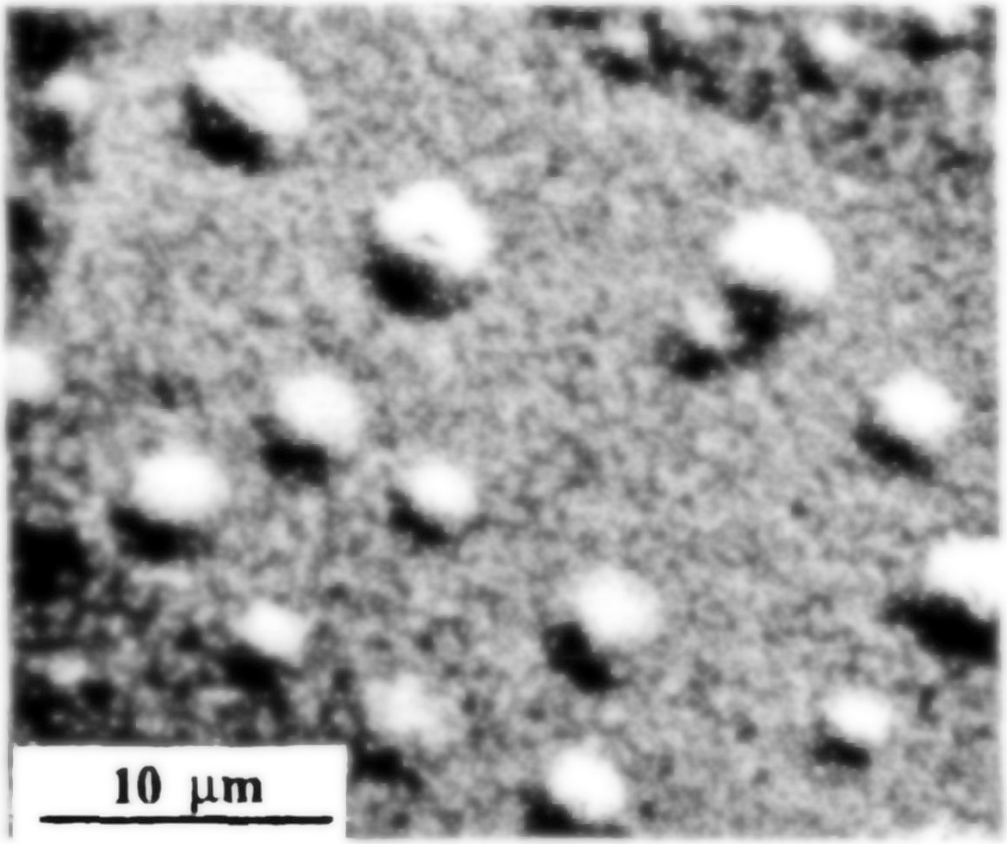

Fig 7. Scanning electron micrograph of a Pt/Ti/SiO_2/Si metallization with Ti= 100 nm annealed in O_2 at 800°C for 2 min, showing encapsulation of Pt with TiO_2.

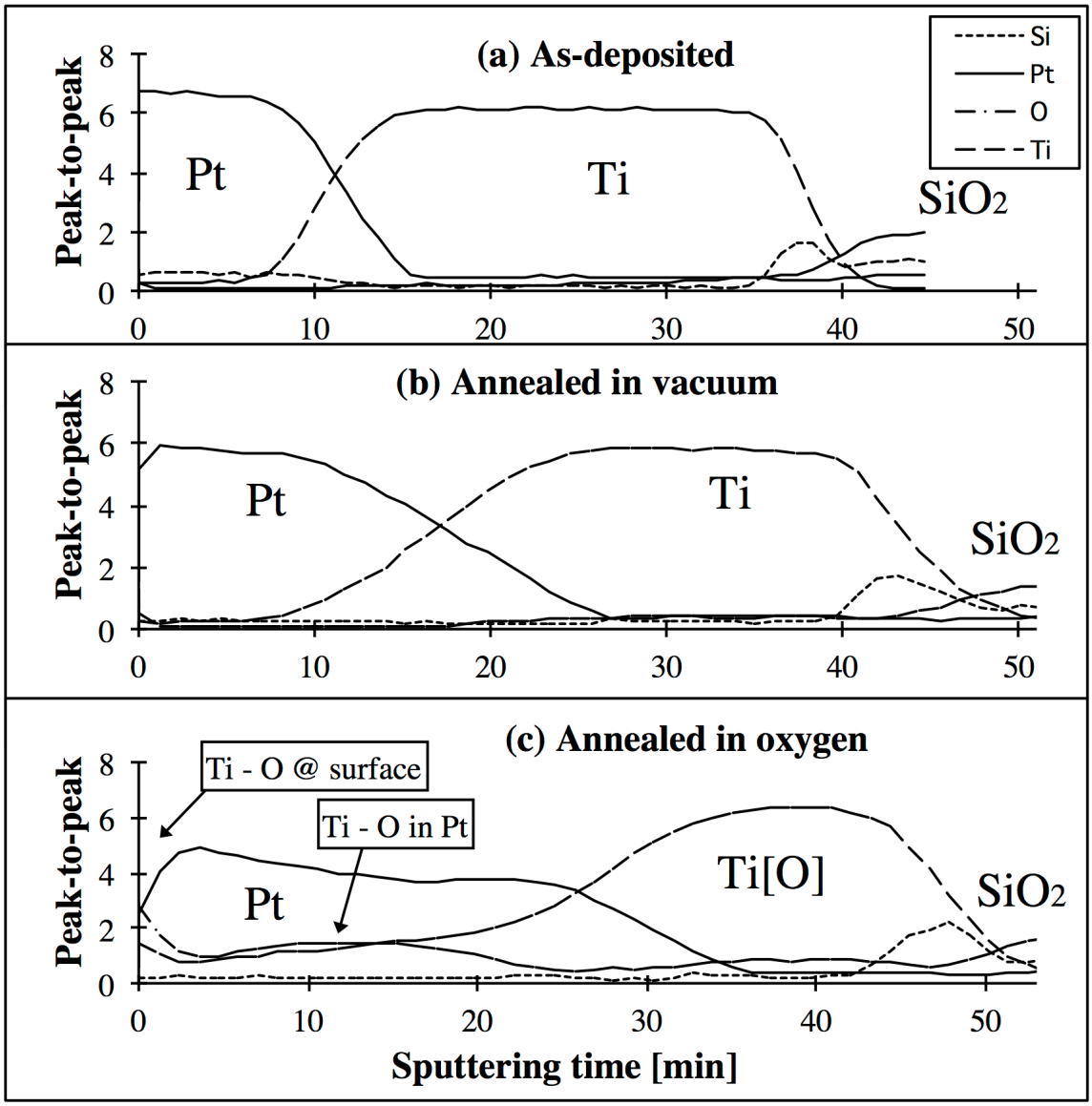

Fig 8. Auger electron spectroscopy (AES) depth profile data on Pt/Ti/SiO_2/Si structures with Ti-100 nm: (a) as-deposited metallization, (b) annealing in vacuum at 650°C for 10 min, (c) annealing in O_2 at 650°C for 10 s.

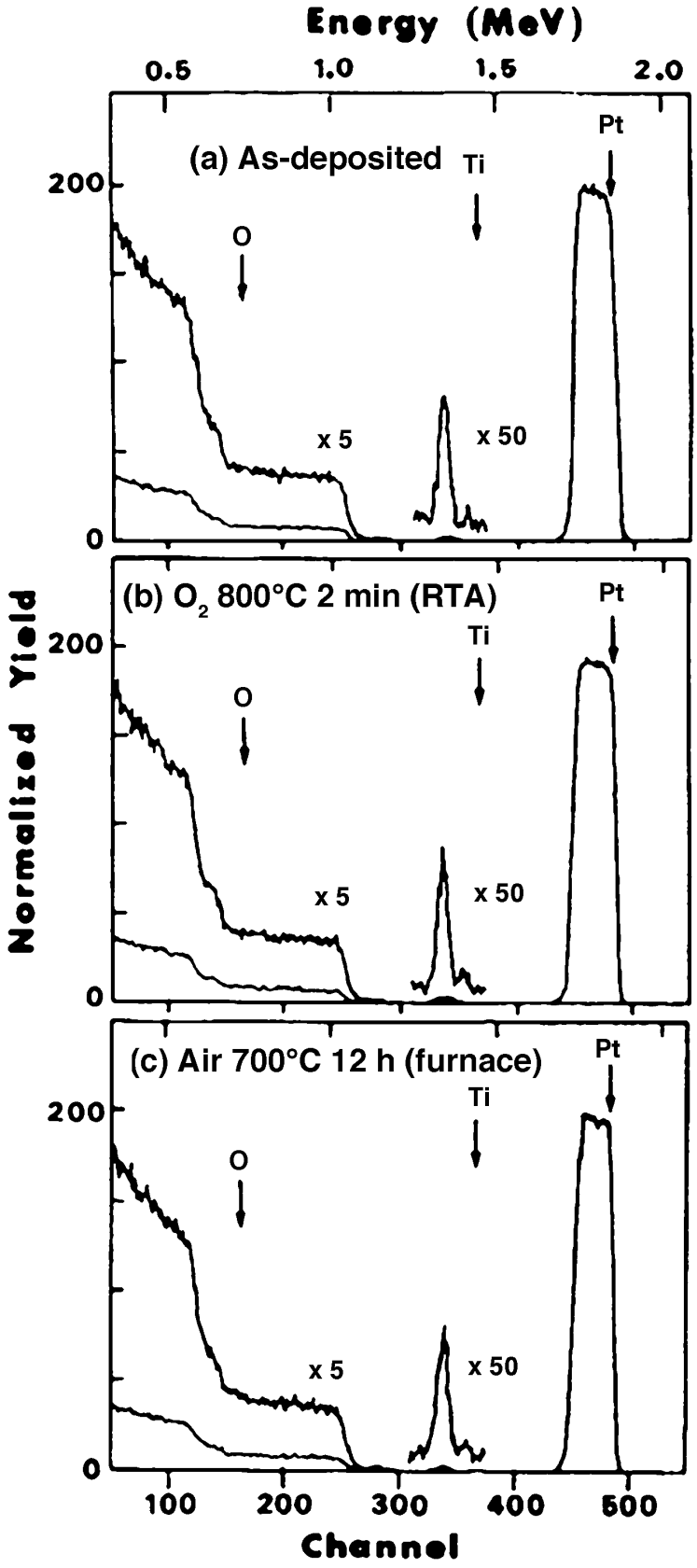

Fig 9. Auger electron spectroscopy (AES) depth profile data on Pt/Ti/SiO_2/Si structures with Ti-100 nm: (a) as-deposited metallization, (b) annealing in vacuum at 650°C for 10 min, (c) annealing in O_2 at 650°C for 10 s.

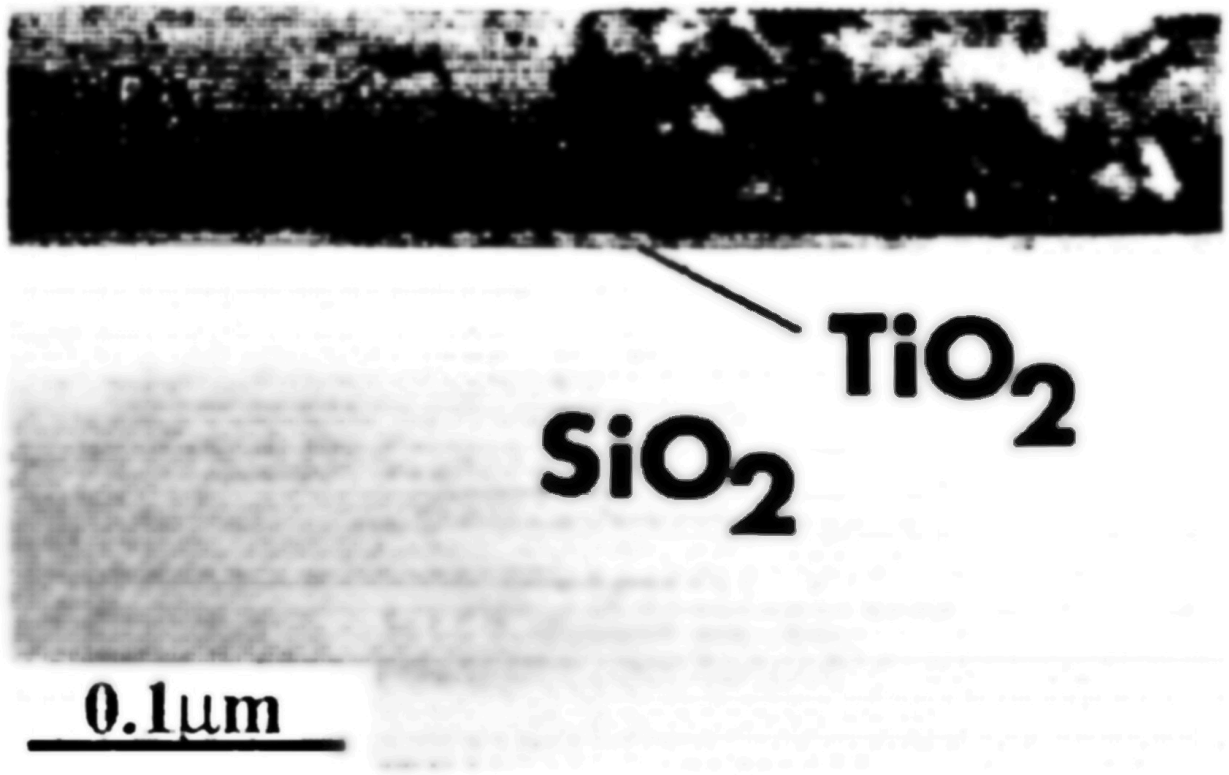

Fig 10. TEM image showing part of a transverse section through the Pt/TiO_2/Ti/SiO_2/Si sample furnace annealed in air at 700°C for 12 h. Thickness (nm): Pt = 71.5, Ti+TiO_2 ~ 6.5 and SiO_2 = 1000.

3.3. Interface reaction mechanisms

The evidence gathered in the present study through RBS, XRD, and TEM studies indicate that the interfacial Ti-bonding layer oxidizes at the same time as migration of Ti occurs in all samples. However, it is not until thick Ti-bonding layers are used that TiO_2 is observed to have encapsulated the Pt surface. Similar observations were reported in earlier studies [13,14], however the encapsulation of the platinum by a thin layer of TiO_2 was not reported, probably due to the lower annealing temperatures (450°C) [14] and the use of very thin Ti layers (< 10 nm) [13]. Encapsulation of a Pt film by a thin layer of TiO_{2-x} has been reported by Sun *et al.* [30]. It was concluded through x-ray photoelectron spectroscopy (XPS) and depth profiling data that encapsulation by TiO_2 occurred predominantly when a Pt film on a reduced TiO_{2-x} single crystal surface was annealed in oxygen. Several mechanisms have been discussed by Spencer [31,32]. Segregation and diffusion of TiO_x in the presence of oxygen were suggested to be thermodynamically favored due to the greater strength of the Ti-O bond (70.0 kcal/mole) in comparison to the Pt-Pt bond (17.7 kcal/mole) and the Pt-Ti bond (22.6 kcal/ mole). Besides the broken bond model, the rapid diffusion and encapsulation of Pt by a thin layer of TiO_{2-x} was attributed to the diffusion of O, and Ti-O through the grain boundaries, and assisted by the mobility in the Pt films [30,33].

In the Pt/Ti bilayer metallizations discussed so far, the depositions were made at a low substrate temperature of 200°C. Such deposition conditions were suspected to produce a platinum film which contained a large number of point defects. This seems to be an inherent property of sputtered coatings, especially when high melting point materials like Pt are deposited at low substrate temperature [3,4]. Such defective layers possess a very small grain size, and tend to re-crystallize during any subsequent thermal treatment with the possibility that point defects may coalesce at the grain boundaries. The defective Pt layers were therefore thought to facilitate the rapid diffusion of oxygen and Ti-O migration through the grain boundaries. An attempt was made to improve the platinum microstructure by depositing the platinum films at a much higher substrate temperature of 500°C.

Pt/Ti bilayer metallizations with 100-nm-thick Ti layers were fabricated with the substrates maintained at a high temperature of 500°C. A separate study was carried out to identify the source of oxygen, and its

effective diffusion path causing the oxidation of the Ti layer. This was accomplished by annealing the samples separately in vacuum and oxygen at identical temperatures (650°C). The AES depth profiles for the as-deposited Pt/Ti metallization [Fig. (8a)] indicated some inter-diffusion at the Pt-Ti interface, but the remaining regions of Pt and Ti maintained their integrity. Reduction of the SiO_2 surface by the Ti layer was observed. In the case of the vacuum annealed sample (650°C for 10 min), the Pt-Ti inter-diffusion zone increased [Fig. 8(b)] in comparison to the as-deposited metallization shown in Fig. 8(a), thus confirming that complete oxidation of Ti did not occur due to the oxygen out-diffusion from the SiO_2. However, annealing in oxygen at 650°C for 10 s indicated the presence of Ti and oxygen throughout the Pt film [Fig. 8(c)] accompanied by the appearance of Ti at the platinum surface.

Increasing the temperature of deposition to 500°C to densify the Pt film was therefore ineffective to prevent the migration of Ti through the Pt film. For further improvement in the stability deposition of a well reacted rutile TiO_2 layer preferably in situ prior to the Pt film deposition was considered. The proposed variation could be implemented by the reactive sputtering of a Ti-metal target in oxygen, and deposition at a high temperature of 650°C (to ensure TiO_2 formation). A thin layer of Ti was deposited before the TiO_2 layer to ensure good adhesion at the Ti-SiO_2 interface.

Metallizations prepared in accordance with the modified Pt/TiO_2/Ti/SiO_2/Si structure were subjected to a thermal treatment in oxygen. Figures 9(a), 9(b), and 9(c) compare the RBS spectra of the as-deposited metallization, the sample annealed in oxygen (700 or 800°C for 2 min), and a sample annealed in air at 700°C for 12 h represented by Fig. 9(c). All RBS spectra shown in Fig. 9 were alike and did not show any significant inter-diffusion indicating a stable Pt-TiO_2 interface. The thicknesses of the various layers noted from the RBS measurements in Fig. 9(a) are as follows: Pt = 80 nm, Ti+TiO_2 = 2 nm and SiO_2 = 900 nm. Figure 10 is a TEM image of the modified Pt/TiO_2/Ti/SiO_2/Si metallization showing a sample annealed for 12 h at 700°C in air. There is no evidence for the presence of pockets of the Ti-rich second phase in the Pt which is well bonded to the TiO_2 layer. The Pt microstructure is columnar with a large grain size. It can be concluded therefore that the metallization was stable with respect to thermal treatments in oxidizing atmospheres at temperatures normally used for the crystallization of ferroelectric thin films.

4. Conclusions

The present investigation presents clear evidence for the deterioration of Pt/Ti bilayer metallizations in oxidizing environments at high temperatures. The interface reactions are complex in nature. Annealing in an oxidizing atmosphere causes oxidation of the intermediate Ti layer and its migration into Pt. This results in the depletion of Ti-bonding material and subsequent loss of adhesion. Use of thicker Ti films caused the formation of TiO_{2-x} in the platinum, and higher annealing temperatures resulted in the ultimate encapsulation of the Pt by a thin layer of TiO_2.

Diffusion of O_2 through the Pt grain boundaries, rapid oxidation of the underlying Ti layers to a reduced TiO_{2-x}, and its subsequent migration into Pt were significant problems. Such adverse reactions could not be prevented despite the deposition of Pt at high temperatures for achieving effective densification in the Pt layers. Improved stability was rather achieved by stabilizing the interface chemistry by incorporating well reacted TiO_2 layers at the interfaces instead of pure metallic Ti thin films. A sequential deposition process combining an in situ sputter cleaning of the substrates, reactive sputtering of Ti in oxygen, and the deposition of Pt films at a high temperature are found to be the critical processing steps for improved stability.

Acknowledgements

This work has been supported by the Swiss National Science Foundation and the Board of Swiss Federal Poly- technic Institutes (CEPF) in the Priority Program on Materials (PPM), The authors gratefully acknowledge Dr. H. J. Mathieu and N. Xanthopoulos for the AES measurements.

References

[1] J. F. Scott and C. A. Paz de Araujo, Science 246, 1400 (1989).

[2] F. P. Gnadinger and D. W. Bondurant, IEEE Spectrum 26, 33 (1989).

[3] R. Ramesh, A. Inam, B. Wilkens, W. K. Chan, D. L.. Hart, K. Luther, and J. M. Tarascon, Science 252, 944 (1991).

[4] D. Bernstein, T. Y. Wong, Y. Kisler, and R. W. Tustison, J. Mater. Res. 8, 12 (1992).

[5] C. B. Eom, R. J. Cava, R. M. Fleming, J. M. Philips, R. B. van Dover, J. H. Marshall, J, W. P. Hsu, J. J. Krajewski, and W. F. Peck, Jr., Science 258, 1767 (1992).

[6] P. D. Wren, S. H. Rou, H. N. Al-Shareef, M. S. Ameen, O. Auciello, and A, I. Kingon, in Proceedings of the 3rd International Symposium on Integrated Ferroelectrics, Colorado Springs, CO, 1991, edited by C. A. Paz de Araujo, pp. 612-625.

[7] N. R. Parikh, J, T. Stephen, M. L. Swanson, and E. R. Myers, in Ferruelectric Thin Films. Vol. 290, MRS Symposium Proceedings, San Francisco, 1990, edited by E. R. Myers and A. I. Kingon (Materials Research Society, Pittsburgh, P.4, 1990). pp. 193-198.

[8] R A. Roy and K. F. Etzold, J. Mater. Res. 7, 1455 (1992).

[9] P. Revesz, J. Li, N. Szabo, Jr., J. W. Mayer, D. Caudillo, and E. R. Myers, in Ferroeiectrie Thin Films-11. Vol. 243, *MRS Symposium Proceedings*, Boston, 1991, edited by E. R. Myers, A. I. Kingon, and R. A. Tuttle (Materials Research Society, Pittsburgh, PA, 1991), pp. 101-106.

[10] I. Kondo, T. Yoneyama, O. Takenaka, and A. Kinbara, J. Vac. Sci. Technol. A 10, 3456 (1992).

[11] G. A. C. M. Spierings, M. J. E, Ulenaers, G. L. M. Kampschöer, H. A. M. van Hal, and P. K. Larsen, J. Appl. Phys. 70, 2290 (1991).

[12] K. Abe, H. Tormita, H. Toyoda, M. Imai, and Y. Yokote, Jpn. J. Appl. Phys. 30, 2152 (1991).

[13] G . A . C. M. Spierings, J. B. A. Van Zcm, M. Klee, and P. K. Larsen, in Proceedings of the 4th International Symposium on Integrated Ferroeletrics, Monterey, CA, March 1992 (in press).

[14] Bruchhaus, D. Pitzer, O. Eibl, U. Scheithauer, and W, Hoester, in Ferroelectric Thin-film-II, Vol. 243, MRS Symposium Proceedings, Boston, 1991, edited by E. R. Myers, A. I. Kingon, and B. A. Tuttle (Materials Research Society, Pittsburgh, PA, 1991), pp. 123-129.

[15] V. Chikramane, J. Kim, C. Sudhama, J. Lee, and Al. Tasch, J. Electron. Mater. 21, 503 (1991).

[16] S. Thakoor, Appl. Phys. Lett. 60, 3319 (1992).

[17] B. A. Tuttle, T. J. Headley, B. C, Bunker, R. W. Schwartz, T. J. Zender, C. L. Hernandez, D. C. Goodnow, R. J. Tissot, J. Michael, and A. H. Carim, J. Mater. Rcs. 7, 1876 (1992).

[18] R. D, Pugh, M, J. Sabochick, and T. E. Luke, J. Appl. Phys. 72, 1049 (1992).

[19] S . S. Dana, K. F. Etzold, and J, Clabes, J. Appl. Phys. 69, 4398 (1991).

[20] L. E. Sanchez, S. Y. Wu, and I. K. Naik, Appl. Phys. Lett. 56. 2399 (1990).

[21] S. B. Krupanidhi and D. Roy, J. Appl. Phys. 72, 620 (1992).

[22] H. Watanabe. T. Mihara. and C. A. Paz de Arauzo, in Proceedings of the 3rd International Symposium on Integrated Ferroelectrics, Colorado Springs, CO, 1991, edited by C. A. Paz de Arauzo, pp. 139-149.

[23] J. O. Olowolafe, R. E. Jones, A, C. Campbell, R. I. EIegde, C. J. Mogah, and R. B. Gregory, J, Appl. Phys. 73, 1764 (1993).

[24] L. R. Doolittle, Nucl. Instrum. Methods B 9, 344 (1985).

[25] K. Sreenivas and M. Sayer, J. Appl. Phys. 64, 1484 (1988).

[26] S. Q. Wang and J. W. Mayer, Thin Solid Films 202, 105 (1991).

[27]. R. Velho and R. W. Bartlett, Metall. Trans. 3, 65 (1972).

[28] Hj. Matzke, in *Non Stoichiometric Oides*, edited by O. Toft Sørensen (Academic, New York, 1981). p. 206.

[29] J. F. Scott, B. M. Melnick, and C. A. Araujo, L. D. McMillan, and R Zuleeg, in Proceedings of the 3rd nternational Symposium on Integrated Ferroelectrics (ISIF), Colorado Springs, CO, 1991, edited by C. A. Paz de Araujo, pp. 176-l84.

[30] Y. M. Sunn, D. N. Belton, and J. M. White, J. Phys. Chem. 90, 5178 (1986).

[31] M. S. Spencer, Surface Science 145, 145 (1984).

[32] M. S. Spencer, Surface Science 145. 153 (1984).

[33] M. S. Spencer, Surface Science 93, 216 (1985).

[34] J. A. Thornton, in Deposition Technologiesfor Films and Coutings,edited by R. F. Bunshah (Noyes, New York, 1982), p. 213.